BBA - Bioenergetics 1864 (2023) 148973

Contents lists available at ScienceDirect

BBA - Bioenergetics

journal homepage: www.elsevier.com/locate/bbabio

Effects of acute cigarette smoke concentrate exposure on mitochondrial energy transfer in fast- and slow-twitch skeletal muscle

Stephen T. Decker [a], Nadia Alexandrou-Majaj [c], Gwenael Layec [a,b,*]

[a] Department of Kinesiology, University of Massachusetts Amherst, USA
[b] Institute for Applied Life Science, University of Massachusetts Amherst, USA
[c] Department of Psychology and Brain Sciences, University of Massachusetts Amherst, USA

ARTICLE INFO

Keywords:
Skeletal muscle
Electron transport chain
Mitochondrial leak
ADP/ATP transport cigarette smoke

ABSTRACT

The mechanisms underlying cigarette smoke-induced mitochondrial dysfunction in skeletal muscle are still poorly understood. Accordingly, this study aimed to examine the effects of cigarette smoke on mitochondrial energy transfer in permeabilized muscle fibers from skeletal muscles with differing metabolic characteristics. The electron transport chain (ETC) capacity, ADP transport, and respiratory control by ADP were assessed in fast- and slow-twitch muscle fibers from C57BL/6 mice ($n = 11$) acutely exposed to cigarette smoke concentrate (CSC) using high-resolution respirometry. CSC decreased complex I-driven respiration in the white gastrocnemius (CONTROL:45.4 ± 11.2 $pmolO_2.s^{-1}.mg^{-1}$ and CSC:27.5 ± 12.0 $pmolO_2.s^{-1}.mg^{-1}$; $p = 0.01$) and soleus (CONTROL:63.0 ± 23.8 $pmolO_2.s^{-1}.mg^{-1}$ and CSC:44.6 ± 11.1 $pmolO_2.s^{-1}.mg^{-1}$; $p = 0.04$). In contrast, the effect of CSC on Complex II-linked respiration increased its relative contribution to muscle respiratory capacity in the white gastrocnemius muscle. The maximal respiratory activity of the ETC was significantly inhibited by CSC in both muscles. Furthermore, the respiration rate dependent on the ADP/ATP transport across the mitochondrial membrane was significantly impaired by CSC in the white gastrocnemius (CONTROL:-70 ± 18 %; CSC:-28 ± 10 %; $p < 0.001$), but not the soleus (CONTROL:47 ± 16 %; CSC:31 ± 7 %; $p = 0.08$). CSC also significantly impaired mitochondrial thermodynamic coupling in both muscles. Our findings underscore that acute CSC exposure directly inhibits oxidative phosphorylation in permeabilized muscle fibers. This effect was mediated by significant perturbations of the electron transfer in the respiratory complexes, especially at complex I, in both fast and slow twitch muscles. In contrast, CSC-induced inhibition of the exchange of ADP/ATP across the mitochondrial membrane was fiber-type specific, with a large effect on fast-twitch muscles.

1. Introduction

Cigarette smoke exposure is a significant risk factor for frailty, sarcopenia, and the development of numerous chronic diseases, causing over 480,000 premature deaths in the United States [1]. Additionally, increased muscle fatiguability [2] and lower exercise tolerance [3] are frequently reported in chronic heavy smokers, which contribute to impaired quality of life. The underlying causes of cigarette smoke-induced exacerbations in fatiguability are multifaceted and include impaired oxygen transport [4,5], deficits in myofiber contractile function [6,7], and mitochondrial dysfunction [8–11].

Mitochondrial alterations elicited by chronic cigarette smoking include substantial changes to their functional characteristics [10,12,13], decreased oxidative enzymes activities [14–16], and enhanced mitochondrial-derived ROS production [14,15,17]. Interestingly, the mechanisms by which energy transduction in the mitochondria of skeletal muscle is directly impaired by cigarette smoke have recently garnered attention. Specifically, acute exposure to cigarette smoke condensate (0.02–1 %) inhibited maximal ADP-stimulated respiration in isolated mitochondria from the hindlimb muscles of mice [18]. In this study, complex-II-supported respiration was also less sensitive to the inhibitory effects of cigarette smoke condensate than

Abbreviations: ADP, Adenosine Diphosphate; ATP, Adenosine Triphosphate; ANT, Adenine Nucleotide Translocase; ETC, Electron Transport Chain; CSC, Cigarette Smoke Concentrate; ROS, Reactive Oxygen Species; CAT, Carboxyatractyloside; FCCP, Carbonyl cyanide-p-trifluoromethoxyphenylhydrazone; COPD, Chronic Obstructive Pulmonary Disease.

* Corresponding author at: Life Sciences Laboratories, 240 Thatcher Rd, Amherst, MA 01003, USA.
E-mail address: glayec@umass.edu (G. Layec).

https://doi.org/10.1016/j.bbabio.2023.148973
Received 6 December 2022; Received in revised form 26 February 2023; Accepted 21 March 2023
Available online 25 March 2023

complex I [18]. Another interesting finding was the documentation of a decreased mitochondrial proton leak with cigarette smoke condensate exposure, which alluded to direct impairment of the electron transport system in this preparation.

Other studies in epithelial cells exposed to cigarette smoke condensate pointed toward an increase in mitochondrial membrane permeability *via* activation of the adenine nucleotide translocase (ANT) [19], a crucial transporter responsible for the exchange of nucleotides (*i.e.*, ADP and ATP) across the inner mitochondrial membrane [20]. ANT also serves as an important site of proton leak and mitochondrial uncoupling [21], regulating mitochondrial membrane potential and the protonmotive force driving ATP production. Based on the above evidence obtained *in vitro* in isolated mitochondria and cultured cells, the impairment of mitochondrial ATP production induced by cigarette smoke in the skeletal muscle can be mediated by three potential mechanisms: decreased supply of reducing equivalent in the electron transport, increased proton leak, and/or decreased ATP turnover (ATP synthesis and transport across the membrane). However, whether all these mechanisms are involved and their relative contribution to the bioenergetic deficits induced by cigarette smoke in the skeletal muscle remains to be established. In addition, given the existence of different mitochondrial phenotypes between fast and slow muscle fibers [22,23], it is also important to determine whether these mechanisms may be fiber-type specific.

The purpose of the present study was to examine the effect of cigarette smoke concentrate on mitochondrial energy transfer involving the electron transport chain, ADP transport into the mitochondria, and respiratory control by ADP in permeabilized fibers from skeletal muscles with differing metabolic characteristics. To achieve these aims, we assessed *in situ* mitochondrial respiration *via* titrations of ADP and carboxyatractyloside, an ANT inhibitor, in predominantly fast (white gastrocnemius) and slow-twitch (soleus) skeletal muscle fibers acutely exposed to cigarette smoke concentrate (CSC) *in vitro*. CSC, a commonly-used substance for the investigation of the effects of cigarette smoke on cellular function *in vitro* [12,18,24–26], and contains the lipid-soluble componenets of cigarette smoke that impact cellular function [12,18] and thus, induce mitochondrial dysfunction *in vitro*. In addition, CSC incubation triggers the fundamental regulatory changes that occur in response to an acute exposure to cigarette smoke, which is crucial to better understand the toxicity of cigarette smoke within the skeletal muscle. We hypothesized that CSC would inhibit the sensitivity and maximal capacity of mitochondrial respiration supported by ADP, attributed to decreased electron flow through the respiratory complexes combined with impairments in ANT activity, resulting in enhanced proton leak.

2. Methods

2.1. Animals and experimental design

Eleven mature C57BL/6 mice (male/female = 7/4) were used for this study. All animals were maintained on a 12-h dark/light cycle without access to running wheels and were fed standard chow *ad libidum*. Following euthanasia by 5 % isoflurane, the white gastrocnemius and soleus were immediately harvested and placed in an ice-cold BIOPS preservation solution [27]. The white gastrocnemius and soleus were specifically chosen to encompass tissues that contain varying amounts of type I and type II skeletal muscle fibers [28], and these two tissues have been shown to recapitulate mitochondrial function observed in humans [29]. Animal use and husbandry followed protocols approved by the University of Massachusetts Institutional Animal Care and Use Committee (IACUC #2152).

2.2. Preparation of permeabilized muscle fibers

The tissue preparation and respiration measurement techniques were adapted from established methods [27,30] and have been previously described by our group [31]. Briefly, BIOPS-immersed fibers (2.77 mM CaK_2EGTA, 7.23 mM K_2EGTA, 50 mM K^+ MES, 6.56 mM $MgCl_2$, 20 mM Taurine, 5.77 mM ATP, 15 mM PCr, 0.5 mM DTT, 20 mM Imidazole) were carefully separated with fine-tip forceps and subsequently bathed in a BIOPS-based saponin solution (50 μg saponin.mL^{-1} BIOPS) for 30 min. Following saponin treatment, muscle fibers were rinsed twice in ice-cold mitochondrial respiration fluid (MIR-05, in mM: 110 Sucrose, 0.5 EGTA, 3 $MgCl_2$, 60 K-lactobionate, 20 taurine, 10 KH_2PO_4, 20 HEPES, BSA 1 g.L-1, pH 7.1) for 10 min each.

Following chemical permeabilization, tissues were incubated *in vitro* for 1-h in separate containers with a 2 mL solution of MiR05 (control) or 4 % (80 μg/mL) cigarette smoke concentrate (CSC; Murty Pharmaceuticals, Lexington, KY) at 4 °C. These concentrations of cigarette smoke concentrate were chosen based on pilot studies (supplementary fig. S2) indicating that this concentration replicates the mitochondrial impairments previously reported in mice and humans chronically exposed to airstream cigarette smoke [8,10,32] and used in previous research by our lab [26].

Immediately after incubation, the muscle sample was gently dabbed with a paper towel to remove excess fluid, and the wet weight of the sample (1–2 mg) was measured using a standard, calibrated scale. The muscle fibers were then placed in the respiration chamber (Oxygraph O2K, Oroboros Instruments, Innsbruck, Austria) with 2 mL of MIR05 solution warmed to 37 °C. Oxygen was added to the chambers, and oxygen concentration was maintained between 190 and 250 μM to prevent O_2 diffusion limitation. After allowing the permeabilized muscle sample to equilibrate for 5 min, mitochondrial respiratory function was assessed in duplicate. Following the addition of each substrate, the respiration rate was recorded until a steady state of at least 30-s was reached, the average of which was used for data analysis. The rate of O_2 consumption was expressed relative to muscle sample mass (in picomoles per second per milligram of wet weight).

2.3. Measurement of mitochondrial respiration

The titration protocol used in the present study was designed to investigate several steps of the mitochondrial energy transduction pathway in permeabilized fibers from the skeletal muscle and was performed as follows: First, saturating concentrations of glutamate (G; 10 mM) and malate (M; 2 mM) were added to the chambers. The addition of glutamate and malate without the presence of ADP (also known as state II/IV respiration) represents a non-phosphorylating state where the oxygen consumed by the mitochondria is linked to the leak of protons out of the mitochondrial intermembrane space [33]. After attaining a steady-state, ADP was added in 5 titration steps: 1) 0.025 mM, 2) 0.05 mM, 3) 0.10 mM, 4) 0.25 mM, and 3) 5 mM (ADP_{5000}) to characterize mitochondrial respiration sensitivity to ADP and maximal ADP stimulated respiration linked to complex I. Following this step, saturating amounts of succinate (S; 10 mM) were added to the chambers to assess maximal complex I & II-driven mitochondrial respiration. Cytochrome c (C; 10 μM) was added to assess the integrity of the outer mitochondrial membrane [34]. Carboxyatractyloside (CAT; Cayman Chemical no. 21120), a selective non-competitive inhibitor of the adenine nucleotide translocator (ANT), was added in 5 steps with final concentrations of 0.05 μM, 0.1 μM, 0.2 μM, 1.0 μM, and 5.0 μM. Following this, carbonyl cyanide *m*-chlorophenyl hydrazone (FCCP) was titrated to assess the capacity of the mitochondrial electron transport chain. Rotenone (Rot; 0.5 μM), a complex I inhibitor, was then added to the chamber to assess complex II-linked respiration. Lastly, oligomycin (Omy; 2.5 μM), an inhibitor of ATP synthase, and antimycin A (AmA; 2.5 μM), a complex III inhibitor, were added to the chambers to assess residual, or non-mitochondrial, oxygen consumption.

2.4. Data analysis

The rate of O_2 consumption (JO_2) was expressed relative to muscle sample mass (in picomoles per second per milligram of wet weight). Samples that demonstrated impaired mitochondrial membrane integrity (more than a 10 % increase in respiration in response to cytochrome C) were excluded from the analysis ($n = 3$). All extreme outliers (more extreme than Q1–3 * IQR or Q3 + 3 * IQR) were also excluded from the analysis. The relative contribution of Complex II to maximal uncoupled respiration was determined by calculating the ratio of Rot:$FCCP_{Peak}$.

Thermodynamic coupling (q) is another method of quantifying mitochondrial respiratory capacity [35] and estimates all enzymatic processes and free energy changes that occur during oxidative phosphorylation. Furthermore, thermodynamic coupling changes are theorized to reflect changes in the P/O ratio [35,36]. Thermodynamic coupling was calculated by:

$$q = \sqrt{1 - \frac{CAT_{5.0}}{FCCP_{\mathrm{Peak}}}}$$

CSC-induced changes to the ETS (Δ $FCCP_{Peak}$) in the white gastrocnemius and soleus was determined by calculating the difference in uncoupled respiration ($FCCP_{Peak}$) between the cigarette smoke concentrate and control tissues expressed as a percentage of the control fibers. CSC-induced inhibition to ANT for each tissue was calculated as follows:

$$\text{CSC} - \text{induced ANT inhibition } (\%) = \frac{(\mathrm{GMDS_{Smoke}} - \mathrm{CAT_{5.0\ Smoke}}) - (\mathrm{GMDS_{Control}} - \mathrm{CAT_{5.0\ Control}})}{\mathrm{GMDS_{Control}}}$$

Apparent K_m and V_{max} were determined using a 3-parameter model of the Michaelis-Menten equation:

$$JO_2 = C + \frac{V_{max} + C}{1 + \frac{K_m}{[S]}}$$

where JO_2 is the respiration rate at the concentration of a given substrate [S], V_{max} is the maximal rate of respiration, K_m is the concentration of [S] at 50 % of V_{max}, and C is JO_2 when [S] = 0. Likewise, the inhibitory kinetics of CAT was fitted to the same equation but modified as follows:

$$JO_2 = I_{max} + \frac{C - I_{max}}{1 + \frac{IC_{50}}{[S]}}$$

where I_{max} is the minimum rate of respiration induced CAT and IC_{50} is the respiration rate at 50 % I_{max}.

Normality and homoscedasticity were determined using the Shapiro-Wilk test and Levene's test, respectively. Due to violations in the assumptions of normality and/or homoscedasticity, the effects of cigarette smoke concentrate and tissue on all parameters were determined using a two-way (CSC×Tissue) Aligned Ranks Transform (ART) ANOVA [37]. If main effects or interaction effects were determined to be statistically significant ($p < 0.05$), *post hoc* comparisons were performed using Dunn's test with a Holm-Sidak correction. Likewise, a nonparametric Wilcoxon's test was used for the comparison between the difference in $FCCP_{Peak}$ between the white gastrocnemius and soleus. Effect sizes were determined by calculating the partial eta-squared (η2) and Cohen's *d* for both the ANOVA and the *post hoc* comparisons, respectively. For clarity, the results are presented as mean ± SD in text and tables, and individual data values in the figures.

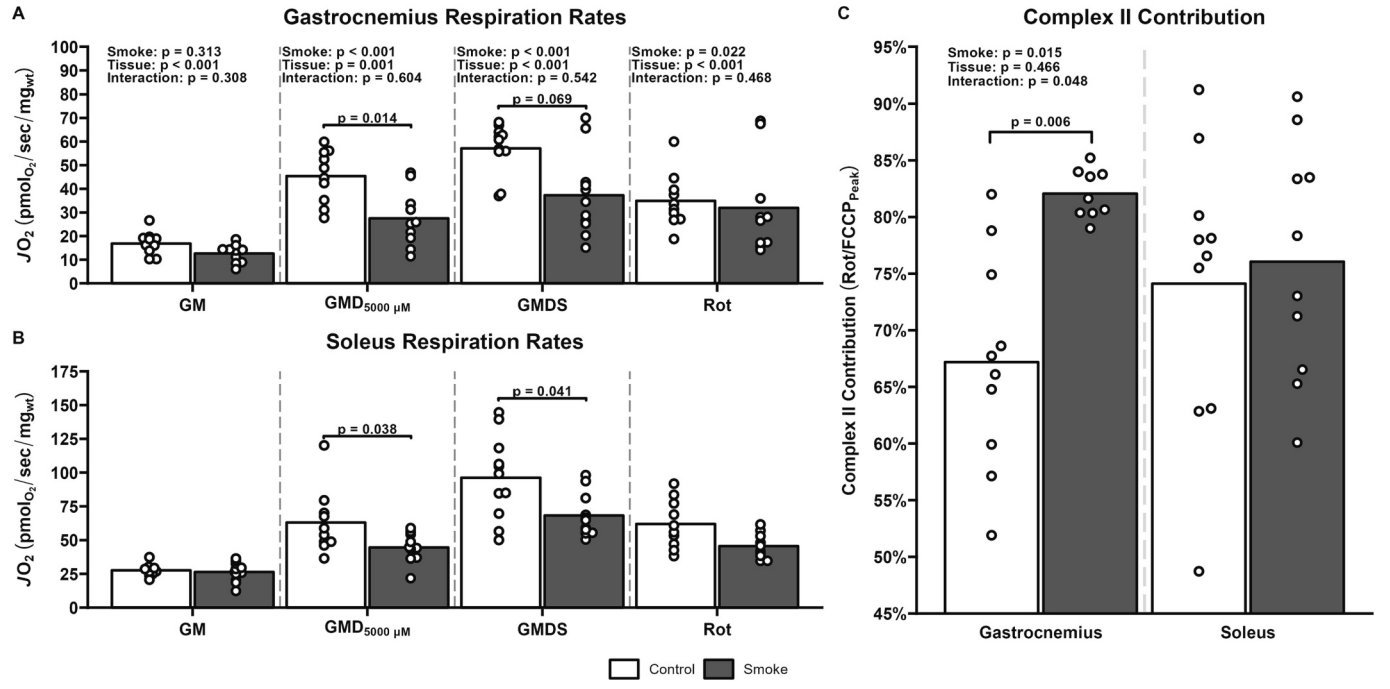

Fig. 1. Respiration rates (JO_2) normalized to the wet weight of permeabilized white gastrocnemius (A) and soleus (B) skeletal muscle fibers incubated in control medium (white bars) or CSC (dark grey bars). Also shown is the contribution of complex II (C). $n = 9$–10 per group. Values are expressed as mean and individual data points. G: glutamate; M: malate; D: ADP; S: succinate; Rot: rotenone.

3. Results

3.1. Effects of CSC on respiratory capacity in fast and slow twitch skeletal muscles

Mitochondrial respiration rates are shown in Fig. 1A and B, and Supplementary Table S1. Leak respiration (GM) was significantly affected by the tissue type ($p < 0.001$, partial $\eta^2 = 0.61$), but not CSC ($p = 0.314$, partial $\eta^2 = 0.03$), nor was there an interaction effect ($p = 0.308$, partial $\eta^2 = 0.03$). Both CSC exposure ($p < 0.001$, partial $\eta^2 = 0.32$) and tissue type ($p = 0.001$, partial $\eta^2 = 0.28$) had main effects on complex-I-driven ADP-stimulated respiration (GMD_{5000}), but there was no interaction effect ($p = 0.604$, partial $\eta^2 = 0.01$). As determined by *post hoc* tests, CSC significantly inhibited the white gastrocnemius (adjusted $p = 0.014$, $d = 1.54$) and soleus muscles (adjusted $p = 0.038$, $d = 0.99$). Likewise, maximal ADP-stimulated respiration (GMDS) with convergent electron flow from complex I and II exhibited significant main effects of CSC ($p < 0.001$, partial $\eta^2 = 0.27$), tissue ($p < 0.001$, partial $\eta^2 = 0.47$), but not an interaction effect ($p = 0.542$, partial $\eta^2 = 0.01$). Maximal ADP-stimulated respiration in CSC-exposed fibers was significantly lower with CSC than control in the soleus (adjusted $p = 0.041$, $d = 1.37$), but only trended toward significance in the white gastrocnemius (adjusted $p = 0.069$, $d = 1.14$).

Complex II-specific respiration, *i.e.* with the addition of rotenone, was affected by CSC ($p = 0.022$, partial $\eta^2 = 0.14$) and tissue type ($p < 0.001$, partial $\eta^2 = 0.37$), but there was not an interaction effect ($p = 0.538$, partial $\eta^2 = 0.01$). There was a significant main effect of CSC ($p = 0.015$, partial $\eta^2 = 0.16$) and an interaction effect ($p = 0.048$, partial $\eta^2 = 0.11$), but no main effect of tissue ($p = 0.466$, partial $\eta^2 = 0.02$) on the relative contribution of complex II respiration (Fig. 1C). *Post hoc* analysis indicated a significant increase in the CSC-exposed white gastrocnemius compared with control (control: 67.2 ± 9.5 %; CSC: 82.1 ± 2.1 %; adjusted $p = 0.006$, $d = 2.16$). No significant differences were observed in the soleus between control and CSC conditions (control: 74.1 ± 12.6 %; CSC: 76.1 ± 10.4 %; adjusted $p = 0.323$, $d = 0.17$).

Effects of CSC on the electron transport chain in fast and slow twitch skeletal muscles.

Uncoupled respiration (FCCP Peak; Fig. 2A) was significantly affected by CSC ($p = 0.003$, partial $\eta^2 = 0.20$) and tissue type ($p < 0.001$, partial $\eta^2 = 0.39$), however, there was not a significant interaction effect ($p = 0.892$, partial $\eta^2 < 0.01$). *Post hoc* analysis trended toward significant differences between the control and CSC-exposed white gastrocnemius (adjusted $p = 0.082$, d = 0.87), but not the soleus (adjusted $p = 0.139$, d = 0.74). There were no significant main effects of CSC ($p = 0.287$, partial $\eta^2 = 0.04$) or tissue ($p = 0.946$, partial $\eta^2 < 0.01$), nor an interaction effect ($p = 0.557$, partial $\eta^2 = 0.02$) on the ratio of GMDS to FCCP (Fig. 2B).

3.2. Effects of CSC on ADP kinetics in fast and slow twitch skeletal muscles

Respiration rates and the corresponding Michaelis-Menten kinetic curves during ADP titration in the white gastrocnemius and soleus muscles are shown in Fig. 3A and B, respectively. There were significant main effects of CSC ($p < 0.001$, partial $\eta^2 = 0.35$) and tissue ($p < 0.001$, partial $\eta^2 = 0.38$), as well as significant interaction effects ($p < 0.001$, partial $\eta^2 = 0.37$) in the apparent K_m of ADP (Fig. 3C). No significant differences were observed between the white gastrocnemius control and white gastrocnemius CSC (adjusted $p = 0.431$, $d = 0.35$), the white gastrocnemius control and the soleus CSC ($p = 0.277$, $d = 1.03$), or the CSC-exposed white gastrocnemius and CSC-exposed soleus (adjusted $p = 0.242$, $d = 0.19$).

Similarly, CSC ($p < 0.001$, partial $\eta^2 = 0.35$) and tissue type ($p < 0.001$, partial $\eta^2 = 0.46$) had significant main effects on the skeletal muscle V_{max} (Fig. 3D); however, there was not a significant interaction effect ($p = 0.813$, partial $\eta^2 < 0.01$). *Post hoc* analysis indicated that V_{max} was lower in the CSC-exposed fibers than control in the white gastrocnemius (control: 44.5 ± 10.8 $pmol_{O2}/s/mg_{wt}$; CSC: 27.3 ± 12.4 $pmol_{O2}/s/mg_{wt}$; adjusted $p = 0.014$, $d = 1.48$) as well as the soleus (control: 64.0 ± 22.2 $pmol_{O2}/s/mg_{wt}$; CSC: 42.7 ± 10.1 $pmol_{O2}/s/mg_{wt}$; adjusted $p = 0.013$, $d = 1.23$).

Effects of CSC on adenine nucleotide transfer in fast and slow twitch skeletal muscles.

Dose-response and fitting curves following titration of carboxyatractyloside are shown for the white gastrocnemius and soleus in Fig. 4A and B, respectively. CSC ($p = 0.004$, partial $\eta^2 = 0.21$) and tissue ($p < 0.001$, partial $\eta^2 = 0.43$) type had significant main effects on the initial rate of respiration before the addition of carboxyatractyloside (Fig. 4C). However, there was not a significant interaction effect ($p = 0.717$, partial $\eta^2 < 0.01$). There were no significant main effects of CSC ($p = 0.644$, partial $\eta^2 < 0.01$) and tissue ($p = 0.516$, partial $\eta^2 = 0.01$), nor a significant interaction effect ($p = 0.581$, partial $\eta^2 = 0.01$) in the apparent IC_{50} of carboxyatractyloside (Fig. 4D). Following maximal inhibition of ANT by carboxyatractyloside, there was no longer a

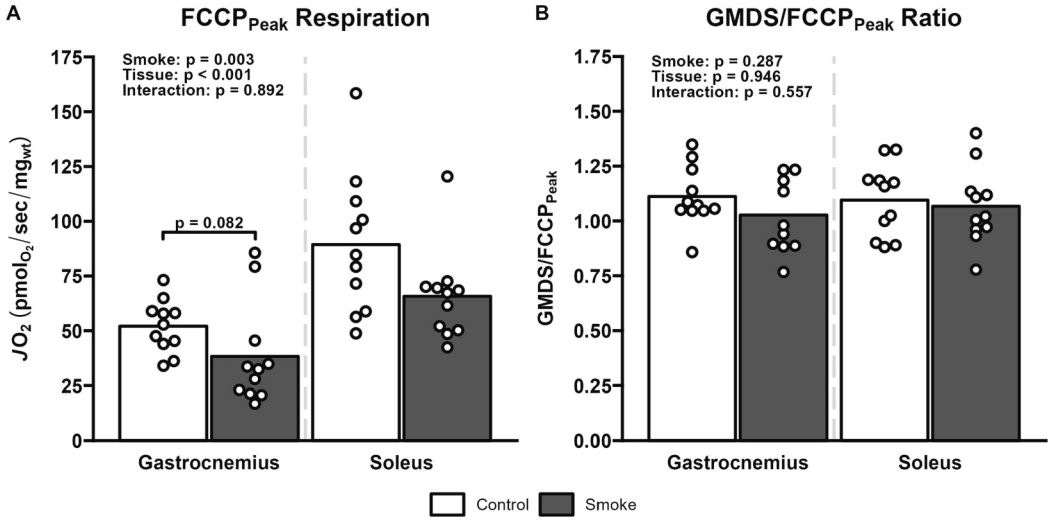

Fig. 2. The smoke-specific effects on uncoupled ($FCCP_{Peak}$) respiration (A) and the ratio of state III coupled respiration (GMDS) to state III uncoupled respiration ($FCCP_{Peak}$; B) in the white gastrocnemius (white) and soleus (grey) muscle fibers. n = 9–10 per group. Values are expressed as mean and individual data points. G: glutamate; M: malate; D: ADP; S: succinate; FCCP: carbonyl cyanide *m*-chlorophenyl hydrazine.

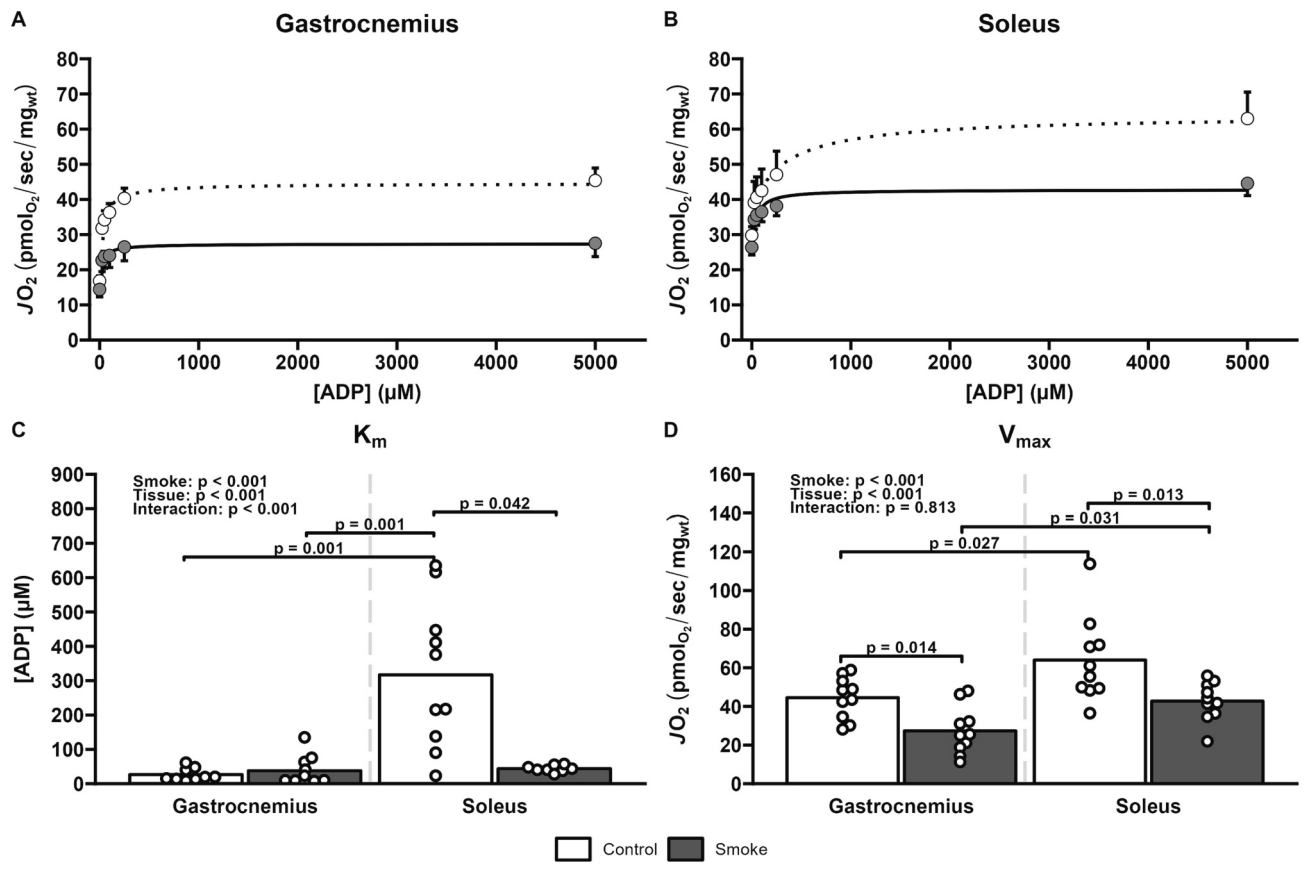

Fig. 3. Dose-response curve for ADP-stimulated respiration in the white gastrocnemius (A; n = 9–10) and soleus (B; $n = 10$) incubated in control medium or CSC (white and grey, respectively); and mean estimates for the apparent K_m (C) and V_{max} (D). Values are expressed as mean ± SEM (panels A and B) and mean with individual data points (panels C and D).

significant main effect of CSC ($p = 0.056$, partial $\eta^2 = 0.10$) or an interaction effect between CSC and tissues on the respiration rate ($p = 0.506$, partial $\eta^2 = 0.01$). There was a significant main effect of tissue type ($p < 0.001$, partial $\eta^2 = 0.41$) on the respiration rate following maximal inhibition by carboxyatractyloside (Fig. 4E).

When data were normalized to the initial respiration rate, the relative inhibition elicited by carboxyatractyloside was significantly attenuated by CSC ($p < 0.001$, partial $\eta^2 = 0.61$), tissue type ($p = 0.048$, partial $\eta^2 = 0.11$), and their interaction ($p = 0.004$, partial $\eta^2 = 0.22$, Fig. 4F). *Post hoc* analysis indicated a significantly lower inhibition of carboxyatractyloside with CSC than control in the white gastrocnemius (control: −70 ± 18 %; CSC: −28 ± 10 %; adjusted $p < 0.001$, $d = 2.96$), and trended toward significance in the soleus (control: 47 ± 16 %; CSC: 31 ± 7 %; adjusted $p = 0.076$, $d = 1.37$).

Relative effects of CSC on the main components of oxidative phosphorylation and indices of mitochondrial efficiency

The CSC-specific inhibition of uncoupled respiration ($FCCP_{Peak}$) for both the white gastrocnemius and soleus are shown in Fig. 5A, which display no significant differences ($p = 0.426$; d = 0.23) between the white gastrocnemius (−29 % ± 30 %) and the soleus (−23 % ± 22 %). The CSC-specific inhibition of ANT is shown in Fig. 5B, which indicates a significant difference ($p = 0.009$; d = 0.93) between the white gastrocnemius (−43 % ± 12 %) and the soleus (−22 % ± 17 %).

Significant main effects of CSC ($p < 0.001$, partial $\eta^2 = 0.58$), tissue ($p = 0.015$, partial $\eta^2 = 0.15$), and an interaction effect ($p = 0.025$, partial $\eta^2 = 0.12$) were observed on the thermodynamic coupling (Fig. 6A). *Post hoc* analysis revealed significant differences between the control and CSC-exposed white gastrocnemius (control: 0.71 ± 0.07, CSC: 0.40 ± 0.15; adjusted $p < 0.001$, $d = 2.70$) and soleus (control: 0.54 ± 0.13, CSC: 0.39 ± 0.12; adjusted $p = 0.046$, $d = 1.18$). Furthermore, there were significant differences between the control white gastrocnemius and control soleus (adjusted $p = 0.042$, $d = 1.74$) and the control white gastrocnemius and the CSC-exposed soleus (adjusted $p < 0.001$, $d = 3.27$). No significant differences were observed between the CSC-exposed white gastrocnemius and the control soleus (adjusted $p = 0.063$, $d = 0.98$) or the CSC-exposed white gastrocnemius and the CSC-exposed soleus (adjusted $p = 0.380$, $d = 0.09$).

4. Discussion

The present study aimed to examine the effect of cigarette smoke concentrate on mitochondrial energy transfer involving the electron transport chain, ADP transport into the mitochondria, and respiratory control by ADP in permeabilized fibers from skeletal muscles with different metabolic characteristics. Consistent with our hypothesis, acute cigarette smoke concentrate exposure significantly inhibited maximal ADP-stimulated respiration in slow- and fast-twitch skeletal muscle fibers. Despite quantitatively similar impairments in maximal ETC capacity, the site of CSC-induced inhibition of mitochondrial respiration appeared to be tissue-dependent. Specifically, the fast-twitch white gastrocnemius muscle exhibited a greater decrease of Complex-I-specific respiration than the slow-twitch soleus. In comparison, Complex II-linked respiration was marginally affected by CSC, such that its relative contribution to muscle respiratory capacity was increased in the CSC-exposed white gastrocnemius muscle relative to controls. CSC also elicited a tissue-dependent effect on respiratory control as mitochondrial respiration sensitivity for ADP was significantly increased in the soleus but not the white gastrocnemius.

Moreover, the effect of carboxyatractyloside-induced inhibition of nucleotide transfer was markedly attenuated in cigarette smoke

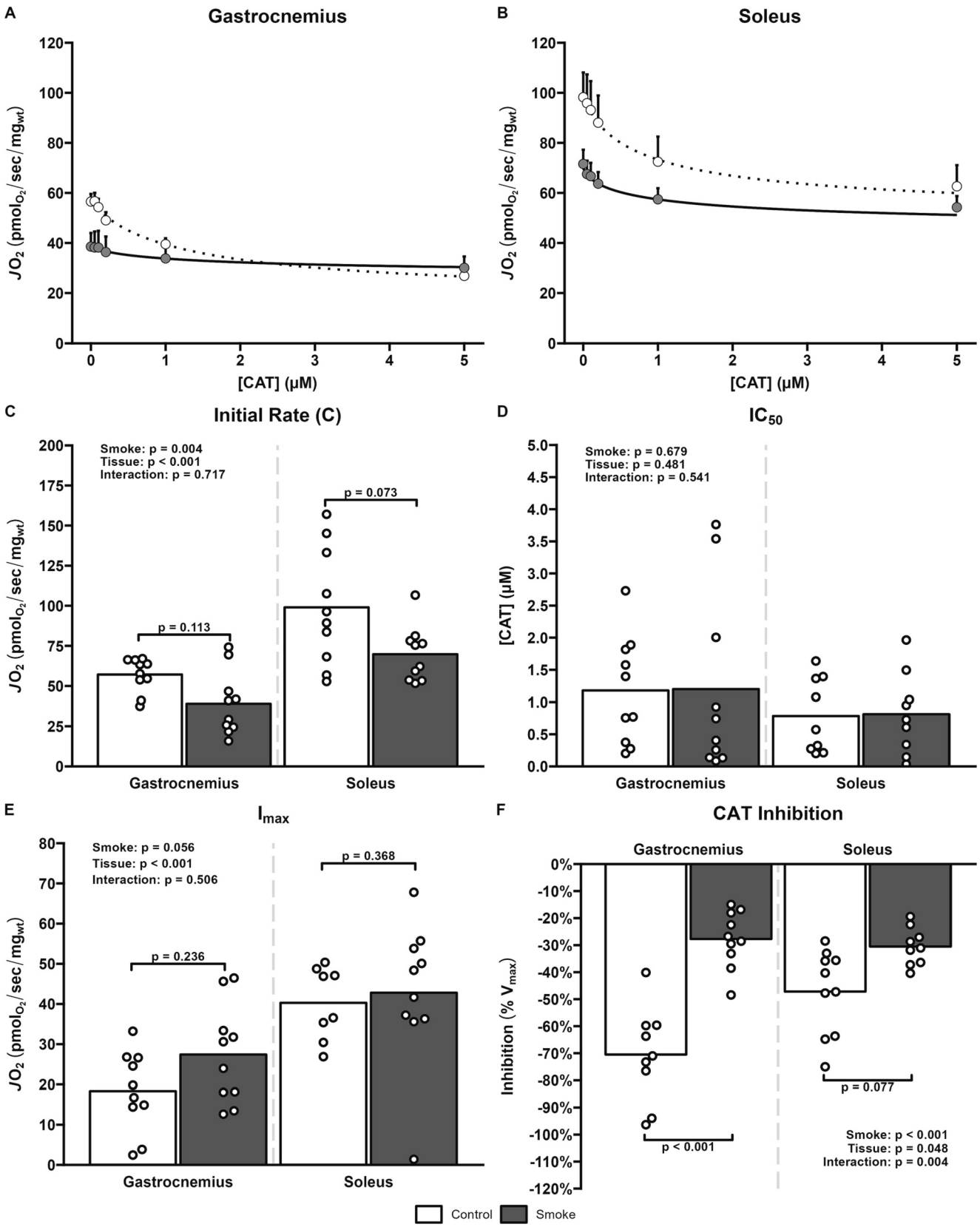

Fig. 4. Dose-response curve for ANT-dependent respiration inhibited by carboxyatractyloside in the white gastrocnemius (A; n = 9–10) and soleus (B; n = 10) incubated in control medium or CSC (white or grey, respectively; *n* = 8–10). Mean estimates for the initial rate (C), apparent IC_{50} (D), I_{max} (E), and the inhibitory effect of CAT relative to the initial rate (F). Values are expressed as mean ± SEM (panels A and B) and mean with individual data points (panels C-F). CAT: Carboxyatractyloside.

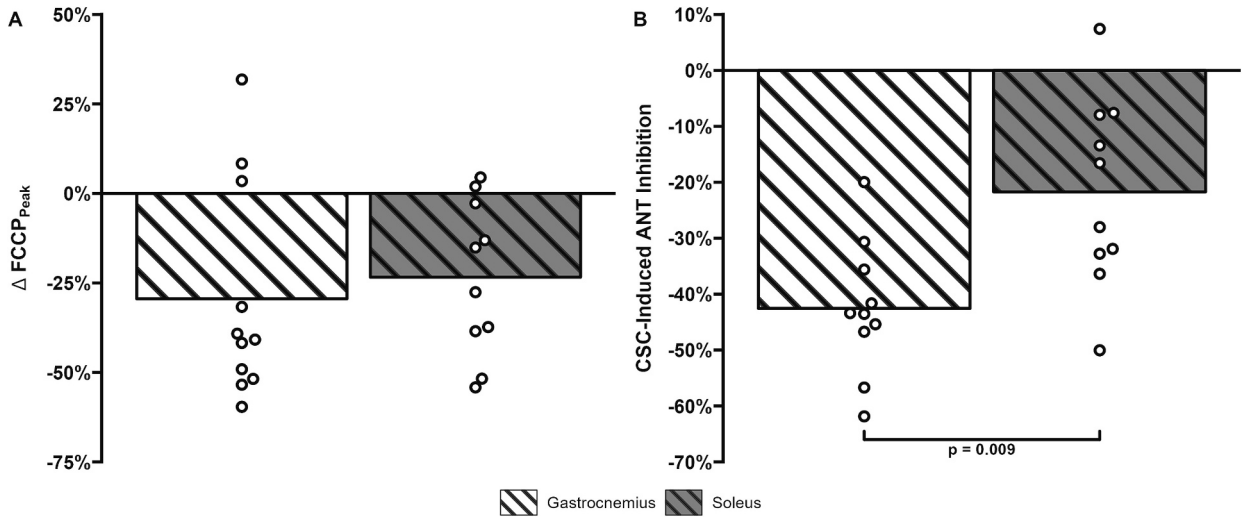

Fig. 5. Cigarette smoke concentrate-induced changes in peak uncoupled respiration ($FCCP_{Peak}$; A; n = 10–11) and the cigarette smoke concentrate-induced inhibition of ANT (B; n = 10). Values are expressed as mean with individual data points. FCCP: carbonyl cyanide *m*-chlorophenyl hydrazine; ANT: adenine nucleotide translocase.

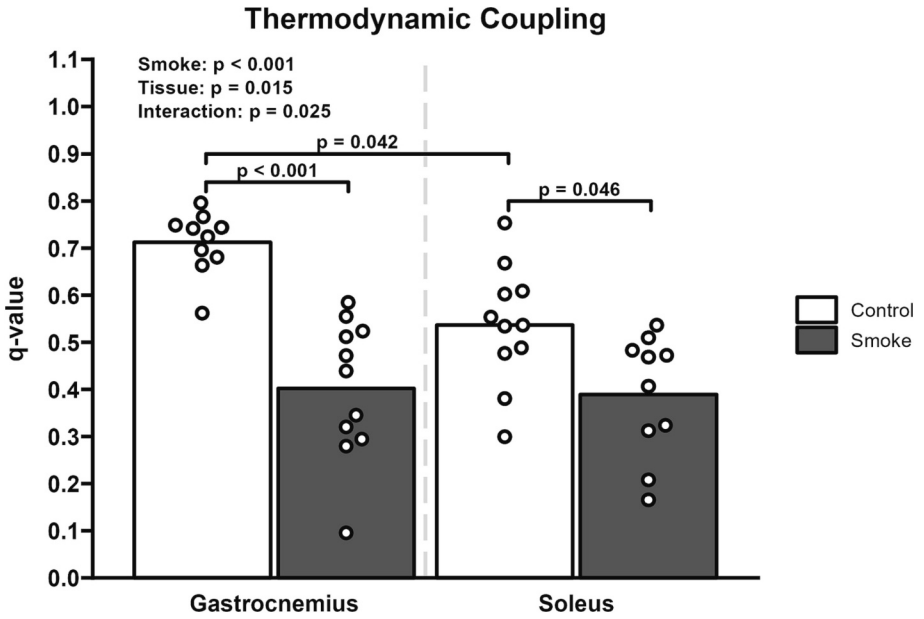

Fig. 6. The thermodynamic coupling of control (white bars, n = 10–11) and cigarette smoke concentrate-exposed (grey bars, n = 10–11) white gastrocnemius and soleus muscle fibers. Values are expressed as mean with individual data points.

concentrate-exposed fibers compared to control tissues, suggesting that cigarette smoke concentrate impairs the ANT-mediated exchange of ATP/ADP across the inner mitochondrial membrane. This mechanism contributed to the cigarette smoke concentrate-induced loss of mitochondrial oxidative capacity and was accentuated in the fast-twitch white gastrocnemius muscle. However, cigarette smoke concentrate did not significantly affect mitochondrial proton leak in slow- and fast-twitch skeletal muscle fibers. Finally, mitochondrial thermodynamic efficiency was decreased by cigarette smoke concentrate in both muscles, albeit with a greater relative decline in the white gastrocnemius than the soleus muscle. Collectively, these findings support the theory that cigarette smoke concentrate directly impairs mitochondrial respiration, especially in fast-twitch muscles. This acute effect was mediated by the inhibition of the mitochondrial ETC capacity, predominantly at the site of complex I, and impairment of nucleotide exchange by ANT in both muscles.

4.1. CSC-induced impairment of muscle respiratory capacity and electron transport chain

Consistent with our hypothesis, CSC drastically inhibited maximal ADP-stimulated respiration with convergent electron flow from complex I and II (GMDS) by ~35 % and ~ 30 % in the white gastrocnemius and soleus muscles fibers, respectively (Fig. 1). When complex I- and II-driven respiration were assessed separately, CSC decreased complex-I-supported respiration by ~40 % in the white gastrocnemius and ~30 % in the soleus. In contrast, the CSC-induced inhibition of complex II-supported respiration was relatively small in both muscles such that the relative contribution of complex II-supported respiration to muscle respiratory capacity was increased with CSC in the white gastrocnemius (Fig. 1C), partially compensating for the decline in mitochondrial membrane potential caused by complex I inhibition. In contrast, the soleus muscle fibers did not demonstrate such compensation of complex

II-driven respiration. Together, these findings suggest that the mechanisms implicated in decreased muscle respiratory capacity following exposure to cigarette smoke concentrate differed between fast and slow twitch muscles. Specifically, the deleterious effect of CSC was mainly mediated by severe complex I inhibition in the fast-twitch white gastrocnemius muscles. In contrast, both complex I- and II-linked respiration were impaired, but to a lower extent, by cigarette smoke concentrate in the slow-twitch soleus muscle. Despite different mechanisms, the cigarette smoke concentrate-induced decline in the capacity for electron transfer through the respiratory complexes was quantitatively similar in fast and slow twitch muscles as uncoupled respiration with the protonophore FCCP was ~25 % lower with CSC in both muscles (Fig. 5A).

Overall, the present findings agree with the results of Khattri et al. [18], which reported a 50–90 % inhibition of complex-I-driven respiration (stimulated by glutamate and malate) in CSC-exposed isolated mitochondria from skeletal muscles of different regions of the body. Likewise, using permeabilized white gastrocnemius muscle fibers, Thatcher et al. [10] reported a ~ 40 % decrease in complex-I-driven mitochondrial respiration in mice exposed to airstream cigarette smoke for six weeks. Although the inhibition induced by cigarette smoke on the respiration rate was evident with both preparations, it is interesting to note the smaller effect size using an *in situ* preparation. Specifically, in the present study, the ~40 % decrease in complex I-supported respiration in the white gastrocnemius muscles following 1 h of 4 % CSC incubation was strikingly similar to the ~40 % decrease in the respiration rate of the red gastrocnemius muscles of mice chronically exposed to airstream cigarette smoke for six weeks [10]. In comparison, mitochondrial respiration in isolated mitochondria from a mixture of skeletal muscles was inhibited by as much as 93 % after exposure to a lower concentration of CSC (1 %) for only 10 min [18]. These findings confirm that mitochondrial isolation procedures exacerbate the susceptibility of the mitochondria to stressors, such as cigarette smoke, whereas the *in situ* preparation more closely recapitulates the extent of mitochondrial dysfunction under conditions that preserve its native morphology [38].

Another important result from the present study was the finding that inhibition of complex I respiration with rotenone significantly attenuated the CSC-induced deficit in mitochondrial respiration, although this effect was fiber-type-specific (Fig. 1C). Indeed, the relative contribution of complex II-supported respiration was higher in the fast-twitch white gastrocnemius muscle after CSC incubation than in control but remained unchanged in the slow-twitch soleus muscle (Fig. 1C). The present findings provide additional insights into the metabolic alterations previously documented in the skeletal muscle of patients with Chronic Obstructive Pulmonary Disease (COPD), a disorder typically caused by chronic cigarette smoking. Specifically, the skeletal muscles of these patients are characterized by a greater proportion of type II muscle fibers in the lower limb [39–41] and a greater reliance on complex II-driven respiration than healthy controls [32,42]. The results of the present study would therefore suggest that this shift in the mitochondrial pathways for energy production in the skeletal muscle of patients with COPD is mediated by the direct effect of cigarette smoke on mitochondrial respiration in type II fibers, which becomes the predominant fiber type as the disease progresses.

4.2. Effect of cigarette smoke concentrate on the control of oxidative phosphorylation in the skeletal muscle

Unlike the white gastrocnemius muscle, the apparent K_m for ADP in the soleus markedly decreased from ~320 μM in the control condition to ~40 μM with CSC (Fig. 3C). In the control condition, the apparent K_m values for ADP for the white gastrocnemius and soleus muscles are within the range of values previously reported using permeabilized muscle fibers. For instance, slow-twitch oxidative muscles are characterized by an apparent K_m for ADP in the range of 200–500 μM whereas fast-twitch glycolytic muscles exhibit values in the range of 10–40 μM [43,44]. This lower sensitivity for ADP in slow-twitch oxidative muscles stems from the selective permeability of the mitochondrial outer membrane to ADP, which restricts its diffusion into the matrix. Interestingly, the mitochondrial sensitivity for ADP of slow-twitch oxidative muscles can be substantially increased (K_m < 100 μM) with the addition of creatine in the respiration buffer [43,44]. In slow-twitch oxidative muscles, mitochondrial creatine kinase (Mt-CK) is functionally coupled to ANT and the voltage-dependent anion channel (VDAC), located on the inner and outer mitochondrial membrane, respectively. Within this functional network, Mt-CK catalyzes the transfer of phosphate groups between the sites of ATP production in the mitochondrial matrix (ATP synthase) and ATP consumption in the cytosol (myosin ATPase and ionic pumps) [45–48].

In light of the Cr/PCr shuttle theory detailed above, the CSC-induced increase in mitochondrial respiration sensitivity for ADP in the permeabilized fibers from the soleus suggests that cigarette smoke concentrate disrupted the functional interactions between VDAC, mtCK, and ANT. This disruption resulted in greater permeability of the mitochondrial outer membrane to ADP in the slow-twitch oxidative muscle, which was, perhaps, mediated by higher VDAC conductance as ANT is unlikely to contribute to this effect (*see next section*). In support of this interpretation, it has been reported that tubulin structure, which is a cytoskeletal protein present at the mitochondrial surface that binds to VDAC and regulates its conductance [49], can be disrupted by cigarette smoke exposure in lung epithelial cells [50]. The present findings provide evidence for a tissue-dependent effect of cigarette smoke concentrate on the control of oxidative phosphorylation mediated by perturbations of the Cr/PCr shuttle in slow-twitch oxidative soleus muscle. Further studies are warranted to examine whether this alteration in the control of oxidative phosphorylation is caused by changes in VDAC conductance.

4.3. Cigarette smoke concentrate-induced perturbation of nucleotide exchange across the mitochondrial membrane

A unique aspect of the present study was the titrations of carboxyatractyloside to examine the effects of cigarette smoke concentrate on the contribution of ANT-mediated exchange of ADP/ATP to mitochondrial respiration. Carboxyatractyloside is a non-competitive inhibitor of ANT [51], which is located on the inner mitochondrial membrane and is responsible for the exchange of ADP/ATP between the mitochondrial intermembrane space and the mitochondrial matrix [20,52], as well as the control of mitochondrial coupling *via* proton leak [21]. CAT binds to the ANT from the cytosolic side of the mitochondrial inner membrane, locking ANT in a cytoplasmic side open conformation and preventing the exchange of ADP/ATP [51,53]. Using CAT to inhibit ANT in the present study, we aimed to measure the functional contribution of ANT to the control of mitochondrial respiration under our experimental conditions.

Using this specific inhibitor ([43,45,54]; V. [46]; V. A. [47,48]), the differences in maximal ADP-stimulated respiration between CSC and control conditions were abolished under saturating concentrations of CAT in the white gastrocnemius and the soleus ($CAT_{5.0}$, Fig. 4E). As a result, the relative inhibition induced by CAT was significantly lower in CSC-exposed fibers (~30 %) than in control fibers (~70–50 %, Fig. 4F) for both muscles, although the magnitude of this effect was tissue-dependent. Specifically, the inhibitory effect of cigarette smoke concentrate on ANT-dependent respiration was markedly higher in the white gastrocnemius (~43 %) than the soleus (~22 %, Fig. 5B). In contrast, cigarette smoke concentrate exposure had no significant effect on the ratio of maximal ADP-stimulated respiration (GMDS) to maximal ETC respiration ($FCCP_{Peak}$, Fig. 2B), which rules out impairments of the phosphorylation capacity of the F_1-F_0 ATP Synthase as a contributor to the decline in maximal ADP-stimulated respiration induced by cigarette smoke concentrate. Collectively, these findings indicate that, in addition

to impairments to the electron transport chain, cigarette smoke concentrate also impaired the exchange of ADP/ATP by specifically inhibiting ANT function. A study in human lung epithelial A459 cells has also previously implicated ANT in the deleterious effects of cigarette smoke concentrate on mitochondrial function [19]. However, the difference in protocols (10 % *versus* 4 % CSC, intact cells *versus* permeabilized fibers, 6 *versus* 1 h incubation, carboxyatractyloside prolonged incubation *versus* acute titration) precluded any direct comparison between the study by Wu et al. and the present work.

Interestingly, the white gastrocnemius was nearly twice as susceptible to CSC-induced ANT inhibition than the soleus muscles (Fig. 5B). Considering the differences in expression of Mt-CK between the white gastrocnemius and soleus muscles [55], it is likely that these observations are due to differing mechanisms which regulate the exchange of adenine nucleotides between the mitochondrial intermembrane space and matrix. Indeed, several models estimate that Mt-CK-facilitated exchange of nucleotides accounts for up to ~80 % of energy transfer from the matrix to the cytosol [49,55–57]. Thus, the Mt-CK present in soleus muscles, which is interdependent on the activity of ANT, could act as a buffer system to better maintain energy transfer between the sarcoplasm and the mitochondrial matrix. Alternatively, the lack of Mt-CK in white gastrocnemius would increase the reliance of these tissues on ANT for energy transfer and, therefore, would increase the susceptibility of the white gastrocnemius to CSC-induced ANT-dependent bioenergetic dysfunction, as observed in the present study.

4.4. Relative effects of cigarette smoke concentrate on the main components of oxidative phosphorylation

Mitochondrial proton leak in slow- and fast-twitch skeletal muscle fibers was not significantly affected by cigarette smoke concentrate, which rules out this mechanism as an important mediator of the effects of cigarette smoke concentrate on mitochondrial function. Also, maximal uncoupled respiration ($FCCP_{Peak}$), in which mitochondrial respiration is not coupled to ATP production and is independent of ADP availability, was less affected by CSC exposure than was maximal coupled respiration (GMDS), thus indicating that additional mechanisms contributed to the inhibition of oxidative phosphorylation capacity. Specifically, maximal coupled respiration was impaired in the CSC-exposed fibers by as much as 40 % and 35 % in the white gastrocnemius and soleus, respectively (Fig. 1A and B). In comparison, uncoupled respiration was only impaired by ~25 % in the white gastrocnemius and soleus under this condition (Fig. 5A). Our results thus support a significant role in the perturbation of ANT-mediated exchange of ADP/ATP to mitochondrial respiration inhibition induced by cigarette smoke concentrate, especially in fast-twitch skeletal muscle fibers.

4.5. Effect of CSC exposure on mitochondrial coupling

Mitochondrial thermodynamic coupling (q-value) was significantly impaired by cigarette smoke concentrate exposure in both muscles (Fig. 6A). Interestingly, the cigarette smoke concentrate-induced loss of energy coupling was accentuated in the fast-twitch white gastrocnemius compared to the slow-twitch soleus muscle. This thermodynamic coupling reflects all enzymatic processes and free energy changes during oxidative phosphorylation [58] and is linked to the mitochondrial P/O ratio [36], thus providing a direct measure of mitochondrial efficiency [35]. The present results in skeletal muscle fibers acutely exposed to cigarette smoke concentrate are consistent with those of Kyle et al. [59], which reported cigarette smoke-induced decreases in the P/O ratio of mitochondria isolated from the lungs of guinea pigs. Also, patients with COPD, a condition caused by chronic cigarette smoking, are characterized by impaired metabolic efficiency during dynamic contraction [60,61].

Conceptually, lower thermodynamic coupling values indicate that mitochondrial respiration was not as tightly coupled to oxidative ATP production following cigarette smoke concentrate exposure, which might be mediated by a greater dissipation of the proton gradient *via* proton leak. However, the lack of significant differences between cigarette smoke concentrate and control conditions in leak respiration (GM, Fig. 1) does not support this mechanism. Alternatively, a decrease in the protons/electrons stoichiometry of the proton pumps caused by slipping of the proton pumps in the respiratory chain [62] may account for the effects of cigarette smoke concentrate on thermodynamic coupling. In support of this interpretation, cigarette smoke concentrate markedly inhibited electron flow in the electron transport chain in both muscles as assessed by the titration of FCCP (Fig. 2A). Also, a lower mitochondrial membrane potential has been consistently documented in various tissue preparation [12,13,17,19], consistent with lower respiratory coupling. From a translational perspective [29,38,59], the impaired efficiency of ATP production in hindlimb skeletal muscles of mice could explain many of the altered bioenergetic differences commonly reported in the locomotor muscles of persons chronically exposed to cigarette smoke, including increased muscle fatiguability [2] and impaired exercise tolerance [3].

4.6. Experimental considerations

Given the low sample size of female mice in the dataset ($n = 4$), and the focus on mitochondrial toxicity *per se*, the present study was ot adequately powered to detect any sex differences in mitochondrial function or any sex-specific effects of cigarette smoke. However, a secondary analysis indicated several nonsignificant trends toward main effects of sex on several of our mitochondrial kinetic parameters (Vmax, relative inhibition of CAT, RCR, thermodynamic coupling, and respiration states with submaximal ADP concentration). It is noteworthy that a recent meta-analysis performed on mitochondrial function in human skeletal muscle fiber bundles reported no overall sex-specific differences in mitochondrial respiration [63]. However, this meta-analysis only analyzed oxygen flux in skeletal muscle mitochondria and did not analyze the sensitivity (K_m) or maximal capacity (V_{max}) to ADP or carboxyatractyloside, presumably due to a lack of studies that have performed these kinetic analyses. Therefore, while the current study was not designed nor powered to identify sex differences in the kinetic parameters of ADP or carboxyatractyloside, our exploratory analysis suggest that future investigation should examine the influence of sex on mitochondrial sensitivity and maximal capacity.

It is also noteworthy that the present study utilized thermodynamic coupling as a surrogate measure of mitochondrial thermodynamic efficiency (P:O ratio) rather than simultaneously measuring ATP production (*via* fluorescence) and oxygen flux directly. Although not a direct measure of mitochondrial efficiency, several studies have shown that thermodynamic coupling is tightly related to the mitochondrial P:O ratio [35,36]. While it is possible to simultaneously monitor ATP flux and oxygen consumption using fluorescent probes and high-resolution respirometry [27,64], these measures have not been validated for use in permeabilized skeletal muscle fiber bundles and, as such, were not available for use in the present study. Thus, once robust methodologies for permeabilized fibers have been rigorously validated, more studies are needed to investigate the effects of cigarette smoke on the mitochondrial P:O ratio in skeletal muscle.

Lastly, the present study sought to investigate the direct effects of cigarette smoke concentrate on mitochondrial ADP sensitivity and ADP/ATP exchange *via* measurement of the activities of ATP synthase and ANT, respectively. However, it is noteworthy that other mitochondrial proteins and pores, such as the mitochondrial permeability transition pore, may become active when exposed to individual constituents of cigarette smoke and may also contribute to impairments in mitochondrial function [65,66]. However, considering that the respiration rate at the maximal inhibition (I_{max}) of carboxyatractyloside was not significantly different between the control and cigarette smoke concentrate-exposed fibers, our data would suggest that the ANT is the

predominent source of increased mitochondrial permeability induced by cigarette smoke concentrate exposure.

5. Conclusion

In conclusion, the present study examined the effects of cigarette smoke concentrate on mitochondrial energy transfer involving the electron transport chain, ADP transport into the mitochondria, and respiratory control by ADP in skeletal muscles with different metabolic characteristics. Acute cigarette smoke concentrate exposure significantly inhibited maximal ADP-stimulated respiration in the skeletal muscle. Interestingly, the site of CSC-induced inhibition of mitochondrial respiration appeared to be tissue-dependent. Specifically, the fast-twitch white gastrocnemius muscle exhibited a greater decrease of Complex-I-specific respiration than the slow-twitch soleus. CSC also elicited a tissue-dependent effect on respiratory control as mitochondrial respiration sensitivity for ADP was significantly increased in the soleus but not the white gastrocnemius.

Furthermore, we provide evidence to suggest that cigarette smoke concentrate also directly impairs mitochondrial thermodynamic efficiency and the exchange of ADP/ATP by inhibiting ANT in the inner mitochondrial membrane. Unlike previous studies using *in vitro* preparation which can affect mitochondrial morphology and function, mitochondrial proton leak in slow- and fast-twitch skeletal muscle fibers was not significantly affected by cigarette smoke concentrate when assessed *in situ* in permeabilized fibers. Our findings shed light on the mechanisms of energy transfer that mediate the cigarette smoke-induced impairment of mitochondrial production of ATP in the skeletal muscle, leading to bioenergetic deficiencies and ultimately contributing to poor exercise tolerance commonly observed in humans chronically exposed to cigarette smoke.

CRediT authorship contribution statement

S.T.D. and G.L. conceived and designed research; S.T.D. and N.A-M. performed experiments; S.T.D and G.L. analyzed data and interpreted results; S.T.D. drafted the manuscript; S.T.D., N.A-M., and G.L. edited and revised the manuscript; S.T.D., N.A-M., and G.L. approved the final version of the manuscript.

Funding

This work was funded by a grant from the NIH National Heart, Lung, and Blood Institute (R00HL125756).

Declaration of competing interest

The authors have no conflict of interest to declare.

Data availability

Data are available upon reasonable request by contacting glayec@umass.edu.

Appendix A. Supplementary data

Supplementary data to this article can be found online at https://doi.org/10.1016/j.bbabio.2023.148973.

References

[1] United States Department of Health and Human Services, The Health Consequences of Smoking—50 Years of Progress A Report of the Surgeon General. A Report of the Surgeon General, 2014.
[2] R.C.I. Wüst, C.I. Morse, A. Haan, J. Rittweger, D.A. Jones, H. Degens, Skeletal muscle properties and fatigue resistance in relation to smoking history, Eur. J. Appl. Physiol. 104 (1) (2008) 103–110, https://doi.org/10.1007/s00421-008-0792-9.
[3] G. Papathanasiou, D. Georgakopoulos, G. Georgoudis, P. Spyropoulos, D. Perrea, A. Evangelou, Effects of chronic smoking on exercise tolerance and on heart rate-systolic blood pressure product in young healthy adults, Eur. J. Prev. Cardiol. 14 (5) (2007) 646–652, https://doi.org/10.1097/HJR.0b013e3280ecfe2c.
[4] C.I. Morse, L.J. Pritchard, R.C.I. Wüst, D.A. Jones, H. Degens, Carbon monoxide inhalation reduces skeletal muscle fatigue resistance, Acta Physiol. (Oxford, England) 192 (3) (2008) 397–401, https://doi.org/10.1111/J.1748-1716.2007.01757.X.
[5] K. Tang, P.D. Wagner, E.C. Breen, TNF-α-mediated reduction in PGC-1α may impair skeletal muscle function after cigarette smoke exposure, J. Cell. Physiol. 222 (2) (2010) 320–327, https://doi.org/10.1002/jcp.21955.
[6] L. Nogueira, B.M. Trisko, F.L. Lima-Rosa, J. Jackson, H. Lund-Palau, M. Yamaguchi, E.C. Breen, Cigarette smoke directly impairs skeletal muscle function through capillary regression and altered myofibre calcium kinetics in mice, J. Physiol. 596 (14) (2018) 2901–2916, https://doi.org/10.1113/JP275888.
[7] P. Robison, T.E. Sussan, H. Chen, S. Biswal, M.F. Schneider, E.O. Hernández-Ochoa, Impaired calcium signaling in muscle fibers from intercostal and foot skeletal muscle in a cigarette smoke-induced mouse model of COPD, Muscle Nerve 56 (2) (2017) 282–291, https://doi.org/10.1002/MUS.25466.
[8] T.T. Ajime, J. Serré, R.C.I. Wüst, G.A.M. Messa, C. Poffé, A. Swaminathan, K. Maes, W. Janssens, T. Troosters, H. Degens, G. Gayan-Ramirez, Two weeks of smoking cessation reverse cigarette smoke-induced skeletal muscle atrophy and mitochondrial dysfunction in mice, Nicotine Tob. Res. (2020), https://doi.org/10.1093/ntr/ntaa016.
[9] S. Pérez-Rial, E. Barreiro, M.J. Fernández-Aceñero, M.E. Fernández-Valle, N. González-Mangado, G. Peces-Barba, Early detection of skeletal muscle bioenergetic deficit by magnetic resonance spectroscopy in cigarette smoke-exposed mice, PLoS ONE (2020), https://doi.org/10.1371/journal.pone.0234606.
[10] M.O. Thatcher, T.S. Tippetts, M.B. Nelson, A.C. Swensen, D.R. Winden, M. E. Hansen, M.C. Anderson, I.E. Johnson, J.P. Porter, P.R. Reynolds, B.T. Bikman, Ceramides mediate cigarette smoke-induced metabolic disruption in mice, Am. J. Physiol. Endocrinol. Metab. (2014), https://doi.org/10.1152/ajpendo.00258.2014.
[11] T.S. Tippetts, D.R. Winden, A.C. Swensen, M.B. Nelson, M.O. Thatcher, R.R. Saito, T.B. Condie, K.J. Simmons, A.M. Judd, P.R. Reynolds, B.T. Bikman, Cigarette smoke increases cardiomyocyte ceramide accumulation and inhibits mitochondrial respiration, BMC Cardiovasc. Disord. 14 (1) (2014), https://doi.org/10.1186/1471-2261-14-165.
[12] M. van der Toorn, D. Rezayat, H.F. Kauffman, S.J.L. Bakker, R.O.B. Gans, G. H. Koëter, A.M.K. Choi, A.J.M. van Oosterhout, D.J. Slebos, Lipid-soluble components in cigarette smoke induce mitochondrial production of reactive oxygen species in lung epithelial cells, Am. J. Physiol. Lung Cell. Mol. Physiol. (2009), https://doi.org/10.1152/ajplung.90461.2008.
[13] M. van der Toorn, D.J. Slebos, H.G. de Bruin, H.G. Leuvenink, S.J.L. Bakker, R.O. B. Gans, G.H. Koëter, A.J.M. van Oosterhout, H.F. Kauffman, Cigarette smoke-induced blockade of the mitochondrial respiratory chain switches lung epithelial cell apoptosis into necrosis, Am. J. Physiol. Lung Cell. Mol. Physiol. (2007), https://doi.org/10.1152/ajplung.00291.2006.
[14] E. Barreiro, L. del Puerto-Nevado, E. Puig-Vilanova, S. Pérez-Rial, F. Sánchez, L. Martínez-Galán, S. Rivera, J. Gea, N. González-Mangado, G. Peces-Barba, Cigarette smoke-induced oxidative stress in skeletal muscles of mice, Respir. Physiol. Neurobiol. (2012), https://doi.org/10.1016/j.resp.2012.02.001.
[15] S.T. Decker, O.S. Kwon, J. Zhao, J.R. Hoidal, T.P. Hueckstedt, R.S. Richardson, K. A. Sanders, G. Layec, T. Heuckstadt, K.A. Sanders, R.S. Richardson, G. Layec, Skeletal muscle mitochondrial adaptations induced by long-term cigarette smoke exposure, Am. J. Physiol. Endocrinol. Metab. (2021), https://doi.org/10.1152/ajpendo.00544.2020.
[16] H.R. Gosker, R.C.J. Langen, K.R. Bracke, G.F. Joos, G.G. Brusselle, C. Steele, K. A. Ward, E.F.M. Wouters, A.M.W.J. Schols, Extrapulmonary manifestations of chronic obstructive pulmonary disease in a mouse model of chronic cigarette smoke exposure, Am. J. Respir. Cell Mol. Biol. (2009), https://doi.org/10.1165/rcmb.2008-0312OC.
[17] G. Haji, C.H. Wiegman, C. Michaeloudes, M.S. Patel, K. Curtis, P. Bhavsar, M. I. Polkey, I.M. Adcock, K.F. Chung, Mitochondrial dysfunction in airways and quadriceps muscle of patients with chronic obstructive pulmonary disease, Respir. Res. 21 (1) (2020), https://doi.org/10.1186/S12931-020-01527-5.
[18] R.B. Khattri, T. Thome, L.F. Fitzgerald, S.E. Wohlgemuth, R.T. Hepple, T.E. Ryan, NMR Spectroscopy Identifies Chemicals in Cigarette Smoke Condensate That Impair Skeletal Muscle Mitochondrial Function, Toxics 10 (3) (2022) 140, https://doi.org/10.3390/TOXICS10030140, 2022, Vol. 10, Page 140.
[19] K. Wu, G. Luan, Y. Xu, S. Shen, S. Qian, Z. Zhu, X. Zhang, S. Yin, J. Ye, Cigarette smoke extract increases mitochondrial membrane permeability through activation of adenine nucleotide translocator (ANT) in lung epithelial cells, Biochem. Biophys. Res. Commun. (2020), https://doi.org/10.1016/j.bbrc.2020.02.160.
[20] M. Klingenberg, The ADP and ATP transport in mitochondria and its carrier, Biochim. Biophys. Acta Biomembr. 1778 (10) (2008) 1978–2021, https://doi.org/10.1016/j.bbamem.2008.04.011.
[21] A.M. Bertholet, E.T. Chouchani, L. Kazak, A. Angelin, A. Fedorenko, J.Z. Long, S. Vidoni, R. Garrity, J. Cho, N. Terada, D.C. Wallace, B.M. Spiegelman, Y. Kirichok, H+ transport is an integral function of the mitochondrial ADP/ATP carrier, Nature 571 (7766) (2019) 515–520, https://doi.org/10.1038/s41586-019-1400-3.
[22] E.J. Anderson, P.D. Neufer, Type II skeletal myofibers possess unique properties that potentiate mitochondrial H(2)O(2) generation, American journal of

physiology. CellPhysiology 290 (3) (2006), https://doi.org/10.1152/AJPCELL.00402.2005.
[23] M. Picard, K. Csukly, M.E. Robillard, R. Godin, A. Ascah, C. Bourcier-Lucas, Y. Burelle, Resistance to Ca2+-induced opening of the permeability transition pore differs in mitochondria from glycolytic and oxidative muscles, Am. J. Physiol. Regul. Integr. Comp. Physiol. 295 (2) (2008), https://doi.org/10.1152/ajpregu.90357.2008.
[24] A. Csiszar, N. Labinskyy, A. Podlutsky, P.M. Kaminski, M.S. Wolin, C. Zhang, P. Mukhopadhyay, P. Pacher, F. Hu, R. De Cabo, P. Ballabh, Z. Ungvari, Vasoprotective effects of resveratrol and SIRT1: attenuation of cigarette smoke-induced oxidative stress and proinflammatory phenotypic alterations, Am. J. Physiol. Heart Circ. Physiol. 294 (6) (2008) 2721–2735, https://doi.org/10.1152/ajpheart.00235.2008.
[25] Z. Orosz, A. Csiszar, N. Labinskyy, K. Smith, P.M. Kaminski, P. Ferdinandy, M. S. Wolin, A. Rivera, Z. Ungvari, Cigarette smoke-induced proinflammatory alterations in the endothelial phenotype: Role of NAD(P)H oxidase activation, Am. J. Physiol. Heart Circ. Physiol. 292 (1) (2007) 130–139, https://doi.org/10.1152/ajpheart.00599.2006.
[26] S.T. Decker, A.A. Matias, S.T. Bannon, J.P. Madden, N. Alexandrou-Majaj, G. Layec, Effects of cigarette smoke on in situ mitochondrial substrate oxidation of slow- and fast-twitch skeletal muscles, Life Sci. 315 (2023) 121376, https://doi.org/10.1016/J.LFS.2023.121376.
[27] D. Pesta, E. Gnaiger, High-resolution respirometry: OXPHOS protocols for human cells and permeabilized fibers from small biopsies of human muscle, Methods Mol. Biol. (2012), https://doi.org/10.1007/978-1-61779-382-0_3.
[28] V. Augusto, C.R. Padovani, G.E.R. Campos, Skeletal muscle fiber types in C57BL6J mice, Braz. J. Morphol. Sci. 21 (2) (2004) 89–94. http://www.jms.periodikos.com.br/journal/jms/article/587cb4537f8c9d0d058b45ea.
[29] R.A. Jacobs, V. Díaz, A.K. Meinild, M. Gassmann, C. Lundby, The C57Bl/6 mouse serves as a suitable model of human skeletal muscle mitochondrial function, Exp. Physiol. (2013), https://doi.org/10.1113/expphysiol.2012.070037.
[30] A.V. Kuznetsov, V. Veksler, F.N. Gellerich, V. Saks, R. Margreiter, W.S. Kunz, Analysis of mitochondrial function in situ in permeabilized muscle fibers, tissues and cells, Nat. Protoc. 3 (6) (2008) 965–976, https://doi.org/10.1038/nprot.2008.61.
[31] G. Layec, G.M. Blain, M.J. Rossman, S.Y. Park, C.R. Hart, J.D. Trinity, J.R. Gifford, S.K. Sidhu, J.C. Weavil, T.J. Hureau, M. Amann, R.S. Richardson, Acute high-intensity exercise impairs skeletal muscle respiratory capacity, Med. Sci. Sports Exerc. (2018), https://doi.org/10.1249/MSS.0000000000001735.
[32] J.R. Gifford, J.D. Trinity, O.S. Kwon, G. Layec, R.S. Garten, S.Y. Park, A.D. Nelson, R.S.S. Richardson, Altered skeletal muscle mitochondrial phenotype in COPD: disease vs. disuse, J. Appl. Physiol. (2018), https://doi.org/10.1152/japplphysiol.00788.2017.
[33] M.D. Brand, D.G. Nicholls, Assessing mitochondrial dysfunction in cells, Biochemical Journal 435 (2) (2011) 297–312, https://doi.org/10.1042/BJ20110162. Portland Press Ltd.
[34] C.G.R. Perry, D.A. Kane, I.R. Lanza, D.P. Neufer, Methods for assessing mitochondrial function in diabetes, Diabetes 62 (2013) 1041–1053, https://doi.org/10.2337/db12-1219.
[35] F.J. Larsen, T.A. Schiffer, S. Borniquel, K. Sahlin, B. Ekblom, J.O. Lundberg, E. Weitzberg, Dietary inorganic nitrate improves mitochondrial efficiency in humans, Cell Metab. 13 (2) (2011) 149–159, https://doi.org/10.1016/J.CMET.2011.01.004.
[36] C.B. Cairns, J. Walther, A.H. Harken, A. Banerjee, Mitochondrial oxidative phosphorylation thermodynamic efficiencies reflect physiological organ roles, Am. J. Physiol. Regul. Integr. Comp. Physiol. 274 (5) (1998) 43–45, https://doi.org/10.1152/AJPREGU.1998.274.5.R1376/ASSET/IMAGES/LARGE/AREG70530005X.JPEG.
[37] J.C. Oliver-Rodríguez, X.T. Wang, Non-parametric three-way mixed ANOVA with aligned rank tests, Br. J. Math. Stat. Psychol. 68 (1) (2015) 23–42, https://doi.org/10.1111/bmsp.12031.
[38] M. Picard, T. Taivassalo, G. Gouspillou, R.T. Hepple, Mitochondria: isolation, structure and function, J. Physiol. 589 (Pt 18) (2011) 4413, https://doi.org/10.1113/JPHYSIOL.2011.212712.
[39] J. Gea, S. Pascual, C. Casadevall, M. Orozco-Levi, E. Barreiro, Muscle dysfunction in chronic obstructive pulmonary disease: update on causes and biological findings, J. Thorac. Dis. (2015), https://doi.org/10.3978/j.issn.2072-1439.2015.08.04.
[40] H.R. Gosker, M.P. Zeegers, E.F.M. Wouters, A.M.W.J. Schols, Muscle fibre type shifting in the vastus lateralis of patients with COPD is associated with disease severity: a systematic review and meta-analysis, Thorax (2007), https://doi.org/10.1136/thx.2007.078980.
[41] A. Nyberg, D. Saey, F. Maltais, Why and how limb muscle mass and function should be measured in patients with chronic obstructive pulmonary disease, Ann. Am. Thorac. Soc. (2015), https://doi.org/10.1513/AnnalsATS.201505-278PS.
[42] J.R. Gifford, J.D. Trinity, G. Layec, R.S. Garten, S.Y. Park, M.J. Rossman, S. Larsen, F. Dela, R.S. Richardson, Quadriceps exercise intolerance in patients with chronic obstructive pulmonary disease: the potential role of altered skeletal muscle mitochondrial respiration, J. Appl. Physiol. (1985) 119 (8) (2015) 882–888, https://doi.org/10.1152/japplphysiol.00460.2015.
[43] Y. Burelle, P.W. Hochachka, Endurance training induces muscle-specific changes in mitochondrial function in skinned muscle fibers, J. Appl. Physiol. 92 (6) (2002) 2429–2438, https://doi.org/10.1152/JAPPLPHYSIOL.01024.2001/ASSET/IMAGES/LARGE/DG0621587005.JPEG.
[44] E. Ponsot, J. Zoll, B. N'Guessan, F. Ribera, E. Lampert, R. Richard, V. Veksler, R. Ventura-Clapier, B. Mettauer, Mitochondrial tissue specificity of substrates utilization in rat cardiac and skeletal muscles, J. Cell. Physiol. 203 (3) (2005) 479–486, https://doi.org/10.1002/JCP.20245.
[45] W. Qin, Z. Khuchua, J. Boero, R.M. Payne, A.W. Strauss, Oxidative myocytes of heart and skeletal muscle express abundant sarcomeric mitochondrial creatine kinase, The Histochemical Journal 31 (6) (1999) 357–365, https://doi.org/10.1023/A:1003748108062, 1999 31:6.
[46] V. Saks, Y.O. Belikova, A.V. Kuznetsov, In vivo regulation of mitochondrial respiration in cardiomyocytes: specific restrictions for intracellular diffusion of ADP, Biochimica et Biophysica Acta 1074 (2) (1991) 302–311, https://doi.org/10.1016/0304-4165(91)90168-G.
[47] V.A. Saks, Z.A. Khuchua, E.V. Vasilyeva, O.Y. Belikova, A.V. Kuznetsov, Metabolic compartmentation and substrate channelling in muscle cells. Role of coupled creatine kinases in in vivo regulation of cellular respiration–a synthesis, Molecular and Cellular Biochemistry 133–134 (1) (1994) 155–192, https://doi.org/10.1007/BF01267954, 2022, Vol. 10, Page 140.
[48] T. Wallimann, M. Wyss, D. Brdiczka, K. Nicolay, H.M. Eppenberger, Intracellular compartmentation, structure and function of creatine kinase isoenzymes in tissues with high and fluctuating energy demands: the "phosphocreatine circuit" for cellular energy homeostasis, The Biochemical Journal 281 (1) (1992) 21–40, https://doi.org/10.1042/BJ2810021.
[49] R. Guzun, M. Gonzalez-Granillo, M. Karu-Varikmaa, A. Grichine, Y. Usson, T. Kaambre, K. Guerrero-Roesch, A. Kuznetsov, U. Schlattner, V. Saks, Regulation of respiration in muscle cells in vivo by VDAC through interaction with the cytoskeleton and MtCK within mitochondrial interactosome, Biochim. Biophys. Acta 1818 (6) (2012) 1545–1554, https://doi.org/10.1016/J.BBAMEM.2011.12.034.
[50] A. Das, A. Bhattacharya, G. Chakrabarti, Cigarette smoke extract induces disruption of structure and function of tubulin-microtubule in lung epithelium cells and in vitro, Chem. Res. Toxicol. 22 (3) (2009) 446–459, https://doi.org/10.1021/TX8002142.
[51] S. Luciani, N. Martini, R. Santi, Effects of carboxyatractyloside a structural analogue of atractyloside on mitochondrial oxidative phosphorylation. Life sciences. Pt. 2: biochemistry, General and Molecular Biology 10 (17) (1971) 961–968, https://doi.org/10.1016/0024-3205(71)90099-3.
[52] E.R.S. Kunji, A. Aleksandrova, M.S. King, H. Majd, V.L. Ashton, E. Cerson, R. Springett, M. Kibalchenko, S. Tavoulari, P.G. Crichton, J.J. Ruprecht, The transport mechanism of the mitochondrial ADP/ATP carrier, Biochim. Biophys. Acta, Mol. Cell Res. 1863 (10) (2016) 2379–2393, https://doi.org/10.1016/J.BBAMCR.2016.03.015.
[53] E. Pebay-Peyroula, C. Dahout-Gonzalez, R. Kahn, V. Trézéguet, G.J.M. Lauquin, G. Brandolin, Structure of mitochondrial ADP/ATP carrier in complex with carboxyatractyloside, Nature 426 (6962) (2003) 39–44, https://doi.org/10.1038/nature02056, 2003 426:6962.
[54] R.L. Barbour, J. Ribaudol, S.H.P. Chanoy, Effect of creatine kinase activity on mitochondrial ADP/ATP transportEvidence for a functional interaction 259 (13) (1984) 8246–8251, https://doi.org/10.1016/S0021-9258(17)39720-X.
[55] T. Wallimann, M. Tokarska-Schlattner, U. Schlattner, The creatine kinase system and pleiotropic effects of creatine, Amino Acids 40 (5) (2011) 1271, https://doi.org/10.1007/S00726-011-0877-3.
[56] M. Aliev, R. Guzun, M. Karu-Varikmaa, T. Kaambre, T. Wallimann, V. Saks, Molecular system bioenergics of the heart: experimental studies of metabolic compartmentation and energy fluxes versus computer modeling, Int. J. Mol. Sci. 12 (12) (2011) 9296, https://doi.org/10.3390/IJMS12129296.
[57] C.G.R. Perry, D.A. Kane, E.A.F. Herbst, K. Mukai, D.S. Lark, D.C. Wright, G.J. F. Heigenhauser, P.D. Neufer, L.L. Spriet, G.P. Holloway, Mitochondrial creatine kinase activity and phosphate shuttling are acutely regulated by exercise in human skeletal muscle, J. Physiol. 590 (Pt 21) (2012) 5475, https://doi.org/10.1113/JPHYSIOL.2012.234682.
[58] J.W. Stucki, The optimal efficiency and the economic degrees of coupling of oxidative phosphorylation, Eur. J. Biochem. 109 (1) (1980) 269–283, https://doi.org/10.1111/j.1432-1033.1980.tb04792.x.
[59] J.L. Kyle, W.H. Riesen, W.H. Riesen, Stress and cigarette smoke effects on lung mitochondrial phosphorylation 21 (4) (2013) 492–497, https://doi.org/10.1080/00039896.1970.10667277.

[60] G. Layec, L.J. Haseler, J. Hoff, R.S. Richardson, Evidence that a higher ATP cost of muscular contraction contributes to the lower mechanical efficiency associated with COPD: preliminary findings, Am. J. Physiol. Regul. Integr. Comp. Physiol. (2011), https://doi.org/10.1152/ajpregu.00835.2010.
[61] R.S. Richardson, B.T. Leek, T.P. Gavin, L.J. Haseler, S.R. Mudaliar, R. Henry, O. Mathieu-Costello, P.D. Wagner, Reduced mechanical efficiency in chronic obstructive pulmonary disease but normal peak VO2 with small muscle mass exercise, Am. J. Respir. Crit. Care Med. 169 (1) (2004) 89–96, https://doi.org/10.1164/rccm.200305-627OC.
[62] D.G. Nicholls, S.J. Ferguson, Bioenergetics, 4th ed., Academic Press, 2013.
[63] A. Junker, J. Wang, G. Gouspillou, J.K. Ehinger, E. Elmér, F. Sjövall, K.H. Fisher-Wellman, P.D. Neufer, A.J.A. Molina, L. Ferrucci, M. Picard, Human studies of mitochondrial biology demonstrate an overall lack of binary sex differences: A multivariate meta-analysis, FASEB J. 36 (2) (2022), https://doi.org/10.1096/FJ.202101628R.
[64] L.H.D. Cardoso, C. Doerrier, E. Gnaiger, Magnesium Green for fluorometric measurement of ATP production does not interfere with mitochondrial respiration, Bioenerg. Commun. 2021 (2021) 1-1, https://doi.org/10.26124/bec:2021-0001.
[65] M. Bonora, C. Giorgi, P. Pinton, Molecular mechanisms and consequences of mitochondrial permeability transition, Nat. Rev. Mol. Cell Biol. 23 (4) (2021) 266–285, https://doi.org/10.1038/s41580-021-00433-y.
[66] L. Puente-Maestu, J. Pérez-Parra, R. Godoy, N. Moreno, A. Tejedor, A. Torres, A. Lázaro, A. Ferreira, A. Agustí, Abnormal transition pore kinetics and cytochrome C release in muscle mitochondria of patients with chronic obstructive pulmonary disease, Am. J. Respir. Cell Mol. Biol. (2009), https://doi.org/10.1165/rcmb.2008-0289OC.